Acanthodian dental development and the origin of gnathostome dentitions

Martin Rücklin[1,2*], Benedict King[1,3], John A. Cunningham[2], Zerina Johanson[4], Federica Marone[5], Philip C. J. Donoghue[2*]

[1]Naturalis Biodiversity Center, Postbus 9517, 2300, RA, Leiden, The Netherlands.
[2]School of Earth Sciences, University of Bristol, Life Sciences Building, Tyndall Avenue, Bristol BS8 1TQ, UK.
[3] Department of Linguistic and Cultural Evolution, Max Planck Institute for Evolutionary Anthropology, Deutscher Platz 6, 04103 Leipzig, Germany.
[4] Department of Earth Sciences, Natural History Museum, Cromwell Road, South Kensington, London SW7 5BD, UK.
[5]Swiss Light Source, Paul Scherrer Institut, CH-5232 Villigen, Switzerland.
*authors for correspondence: martin.rucklin@naturalis.nl; phil.donoghue@bristol.ac.uk
ORCID: MR, 0000-0002-7254-837X; BK, 0000-0002-9489-8274; JC, 0000-0002-2870-1832; ZJ, 0000-0002-844-6776; FM, 0000-0002-3467-8763; PCJD, 0000-0003-3116-7463

Chondrichthyan dentitions are conventionally interpreted to reflect the ancestral gnathostome condition but interpretations of osteichthyan dental evolution in this light have proven unsuccessful, perhaps because chondrichthyan dentitions are equally specialized, or else independently evolved. Ischnacanthid acanthodians are stem-Chondrichthyes; as phylogenetic intermediates of osteichthyans and crown-chondrichthyans, the nature of their enigmatic dentition may inform homology and the ancestral gnathostome condition. Here we show that ischnacanthid marginal dentitions were statodont, composed of multicuspidate teeth added in distally-diverging rows and through proximal superpositional replacement, while their symphyseal tooth whorls are comparable to chondrichthyan and osteichthyan counterparts. Ancestral state estimation indicates the presence of oral tubercles on the jaws of the gnathostome crown-ancestor; tooth whorls and/or tooth rows evolved independently in placoderms, osteichthyans, ischnacanthids, other acanthodians and crown-chondrichthyans. Crown-chondrichthyan dentitions are derived relative to the gnathostome crown-ancestor which possessed a simple dentition and lacked a permanent dental lamina which evolved independently in Chondrichthyes and Osteichthyes.

The dentitions of most modern chondrichthyans (Elasmobranchii: sharks, rays) are organized into files of replacement teeth arrayed side-by-side along the jaw. The simplicity of this conveyor-belt system has long been interpreted to reflect the ancestral condition for the dentitions of jawed vertebrates and theories of dental developmental evolution have invariably attempted to rationalize the dentitions of osteichthyans on such a model[1,2]. Critical to this model is the presence of a permanent dental lamina along the jaw which is responsible for tooth development and replacement, which can be observed in living jawed vertebrates[3-6] and inferred from evidence of comparable tooth replacement patterns in extinct relatives. However, the first fossil evidence of crown-chondrichthyan divergence is from the end-Middle Devonian, later than the first crown-osteichthyans which are late Silurian[7]. Furthermore, recent fossil discoveries have decisively overturned the view that chondrichthyan morphology is representative of the ancestral gnathostome condition[8,9]. The extinct acanthodians are recognized as a paraphyletic lineage of stem chondrichthyans[8] and, as phylogenetic intermediates of the crown-chrondrichthyans and osteichthyans, they have the potential to inform the nature of the dentition in the ancestral crown-gnathostome and, indeed, address the question of whether it possessed a dentition at all[10]. Acanthodians exhibit variation in their dentitions, from acanthodids and diplacanthids which lack teeth entirely, climatiids whose dentition was comprised wholly of statodont tooth whorls, to ischnacanthids that possessed symphyseal tooth whorls, a marginal dentition[11,12] and tooth-like scales around the jaw margins[13,14]. Here we focus on the nature of the dentition in ischnacanthids which manifest the diversity of dentitions seen in dentate acanthodians.

The development of the marginal dentition of ischnacanthids has been interpreted based on its external morphology[12,15] , broken surfaces[16] and a few traditional destructive studies e.g.[14,17]. These data have led to divergent interpretations of the development of the marginal dentition (and therefore its homologies). It has been argued that acanthodian marginal dentitions were shed and replaced *in toto*[18] or that they grew episodically with the teeth developing as continuous projections of the underlying bony plate[19]. Confirming either of these hypotheses would reveal tooth development mechanisms without parallel in other gnathostomes, thereby expanding our knowledge of the disparity of early dentitions. A third hypothesis is that each of the cusps (regardless of size) represent distinct teeth that were added sequentially, extending the tooth row distally[20]. This invites comparisons with arthrodire placoderms (and to a lesser extent osteichthyans), raising the possibility that such dentitions are ancestral for gnathostomes as a whole, or that similar dentitions appeared multiple times through convergent evolution. To discriminate among these interpretations we used SRXTM[21] to study the structure and infer the development of the marginal and

symphyseal dentitions of ischnacanthid acanthodians based on exceptionally-preserved material from the Lower Devonian (Lochkovian) of Prince of Wales Island, Arctic Canada.

Acanthodian jaws consist of paired upper palatoquadrate cartilages and paired lower Meckel's cartilages that were only rarely ossified (perichondrally) and therefore, preserved. The marginal dentition of ischnacanthids is associated with the oral side of these upper and lower jaw cartilages and comprises a more or less extensively developed ossification including oral tubercles. The tubercles are organized into two or more rows that diverge distally at about 20° within a horizontal plane, the first approximately parallel to the jaw margin and the second extending lingually in a distal direction (relative to the jaw joint, Fig. 1c, d, f). A ridge occurs between the rows of tubercles, increasing in prominence distally (Fig. 2c, d).

Tomographic data demonstrate that these oral, tooth-like tubercles developed separately from the bony base to which they are ankylosed (cf. [16]). The bony base is comprised of cancellar cellular bone exhibiting frequent spheritic mineralisation (Fig. 1d,e), overlying a layer of compact lamellar bone. Each of the overlying tubercles has a prominent conical central cusp and a number of smaller accessory cusplets (Fig. 1c, d; 2c); these increase in size distally. A thin (5- 70µm) surface layer of highly attenuating hypermineralised tissue that we interpret as enameloid, extends across the large central cusp and the smaller marginal cusplets, evidencing their formation as a single morphogenetic unit (Fig. 1i), rather than as separately developing tubercles (cf. [12]). The tubercles are otherwise composed of dentine with tubuli extending from a large central pulp-cavity to near the tubercle surface, into the hypermineralised enameloid layer (Fig. 1i). The tubercles in the marginal dentition are therefore compositionally, developmentally and topologically compatible with teeth.

The overlapping relationships of the teeth, delimited by growth arrest lines, allow the development of the dentition to be reconstructed (Figs 1d, f, 2, 3; Extended Data Fig 1). The teeth were added sequentially along a proximal to distal vector within each row, as revealed by their overlapping relationship, with each tooth added onto the distal margin of the predecessor. This proximal to distal sequence is also evidenced by the differing degree to which the pulp cavities have been infilled by centripetal layers of dentine. Teeth within the lateral row are overlapped marginally by teeth within the lingual row (Fig. 1g), indicating that the lateral teeth developed earlier and more distally. This arrangement breaks down proximally where teeth exhibit considerable wear and are replaced through superpositional apposition, though they cannot be assigned to any particular row with confidence (Figs 1f, h, 2, 3; Extended Data Fig 1). We find no evidence for tooth resorption and our data allow us to

reject hypotheses that (a) the dentigerous jawbones of ischnacanthids were episodically shed and replaced in toto[18], (b) the teeth developed episodically as elaborations of the underlying bone[19], and (c) each cusp and cusplet constitutes a developmental unit distinct from the principal cusp[20].

The structure of the tooth whorls is quite distinct, comprised of monocuspid conical teeth that project from a concave oval base and exhibit an ordered increase in height and width lingually. One row of teeth and paired marginal teeth may occur within any one tooth whorl, reducing in height laterally (Fig. 4). The teeth are distinct from the underlying bony base which is composed of a layer of cancellar bone on a thin base of compact lamellar bone (Fig. 4c). Each tooth is composed largely of dentine surrounding a central pulp cavity and a thin (10-50 µm) capping hypermineralised enameloid layer that does not extend to encompass adjacent (successional and marginal) teeth (Fig. 4b). Cancellar bone attaches each tooth to the bony base and the lingual margin of the preceding tooth. Successive teeth are distinguished by a growth arrest line indicating that the largest teeth were added last (Fig. 4b). There is no evidence of apposition of the tooth and its underlying bony base indicating that the two developed synchronously. A network of vascular canals connects the teeth and the dental pulp cavities exhibit polarised pattern of infilling, with the earliest being completely infilled (Fig. 4b).

Ischnacanthid tooth whorls are comparable to the tooth families of living chondrichthyans to which they have long been compared, but they are even more similar to the statodont tooth whorls of other acanthodian stem-chondrichthyans (e.g. *Climatius*, *Ptomacanthus*) and the symphyseal tooth whorls of stem- and early crown-osteichthyans (e.g. *Onychodus*)[22,23] which also possess a unifying bony base[24] and multiple rows of cusps. However, osteichthyan tooth whorls exhibit distinct growth of the teeth and bony base[23].

The marginal dentitions of ischnacanthids find no counterpart in living chondrichthyans in terms of their association with an ossified mandibular plate, their pattern of addition along the jaw rather than across it, or their pattern of dental replacement. They may be compared to the marginal dentitions of arthrodiran placoderms[25] and osteichthyans (e.g. *Onychodus*, *Moythomasia*) in being arranged in marginal rows. In contrast to arthrodiran placoderms and osteichthyans in which tooth addition occurs in both a proximal and distal direction[26,27], the ischnacanthid marginal dentition shows only distal extension of the tooth rows. Our data evidences tooth replacement at the proximal end of the row but, unlike in osteichthyans, this occurs superpositionally and without resorption in ischnacanthids. Thus, while the tooth whorls of dentate acanthodians support inference of a permanent dental lamina, the pattern

of superpositional replacement in the dentigerous jaw bones is incompatible with tooth development within a permanent dental lamina, similarly inferred for stem-osteichthyans[25,28].

Inferring the nature of the ancestral crown-gnathostome dentition requires resolution of homology among diverse gnathostome dentitions, including those of ischnacanthids. This is a question not merely of structural and developmental similarity, but of phylogenetic congruence[29], which is complicated by the uncertainty of phylogenetic relationships among early gnathostomes and acanthodians, in particular. Accounting for this uncertainty, we estimated ancestral states for dental characteristics on the posterior distribution trees from a tip-dated Bayesian analysis of early gnathostome relationships (Figs 5, 6). This recovered strong support for the presence of oral tubercles on jaw cartilages in the ancestral crown-gnathostome (Fig. 5, pp=0.99), and homology of osteichthyan and (conventionally-defined) chondrichthyan[8] teeth as oral tubercles (pp=0.95). Loss of oral tubercles is inferred several times in acanthodians (Fig. 5). Testing homology of arthrodiran, osteichthyan and ischnacanthid dentitions, there is evidence for the convergent evolution of marginal tooth rows (Fig. 6a) and tooth whorls among gnathostomes (Fig. 6b). The highest posterior density interval for the number of independent tooth whorl origins was 6-15, and 3-7 for marginal tooth rows. These results are robust to the phylogenetic position of ‘psarolepid’ osteichthyans (Extended Data Fig 2), the status of placoderms as paraphyletic or monophyletic and different divergence dating methodologies (Extended Data Fig 3).

Our results suggest that the ancestral crown-gnathostome possessed teeth. However, complex dentitions, a permanent dental lamina and coordinated tooth replacement, all evolved multiple times; teeth were also lost multiple times among acanthodians (Figs 5, 6). The similarities reported here between tooth rows in ischnacanthid dentitions and those of arthrodiran placoderms and osteichthyans, are inferred to reflect convergence rather than homology (contra [25]). The diversification of crown-gnathostomes is associated with an extremely rapid burst of phenotypic evolution[30] manifest in the diversity of early crown-gnathostome dentitions. This may go some way to explain why models of tooth replacement based on crown-chondrichthyans are such a poor explanatory model for the dentitions of crown-osteichthyans, as well as differences which at least in part inspired the hypothesis that teeth evolved independently within these and other lineages of jawed vertebrates[10,31].

Methods

Museum repository abbreviation: Naturhistoriska Riksmuseet, Stockholm (NRM) and National History Museum London (NHMUK).

Material: Fossil material comprises specimens of an ischnacanthid acanthodian from the Lochkovian, Early Devonian, Prince of Wales Island, Canada. Mandibles with tooth rows: NRM-PZ P. 9449: labeled model (Figs 1b-h, 2). Tooth whorls: specimen figured in Rücklin et al. (2011)[32] from the same locality (NRM-PZ P. 15908, Fig. 3a-c). Ischnacanthid acanthodian jaw from the Downtonian, Upper Silurian, Baggeridge Colliery, South Staffordshire, UK (NHMUK PV P.15362, Fig. 1a)[33].

Tomography: Material from Canada was acid prepared and scanned using SRXTM[21] at the TOMCAT (X02DA) beamline[34] of the Swiss Light Source (SLS), Paul-Scherer Institut, Switzerland. Using a 10x objective 1501 projections were acquired equi-angularly over 180°. Projections were post-processed and rearranged into flat- and darkfield-corrected sinograms, and reconstruction was preformed on a Linux PC farm resulting in isotropic voxel dimensions of 0.74 µm. The complete jaw BMNH P. 15362 was scanned using an x-tex XTH 225ST scanner at Nikonmetronics, Tring. 3142 projections were acquired and were post-processed resulting in isotropic voxel dimensions of 100 µm. Slice data were analysed and manipulated using Avizo 8.01 (www.fei.com). Sectional images were studied and three-dimensional models of the different growth stages were derived segmenting following lines of arrested growth.

Phylogeny and ancestral state reconstruction: The phylogenetic data matrix was based on King et al. [30], with a revised taxon and character list incorporating new information on stem chondrichthyans[14,35,7], and improved sampling of sarcopterygian osteichthyans. The analysis was a tip-dated approach performed in BEAST2.5.2[36] with BEAGLE likelihood calculation library[37]. Characters were partitioned according to the number of states. We applied the Mkv model[38], gamma distributed among-character rate variation, the sampled ancestor birth-death model[39] and the Lognormal relaxed clock[40]. Fossil ages were assigned uniform priors across the range of uncertainty. Analyses were run for 200 million generations with 2000 trees saved. Convergence was assessed in Tracer[41] and RWTY[42]. The analysis strongly supports a sarcopterygian position for the 'psarolepid' osteichthyans, but as previously discussed, this may be an artefact of the relatively sparse coding for the characters supporting a stem osteichthyan position for these taxa[43]. Therefore a second analysis was performed in which they were contstrained to be stem osteichthyans. We utilised a backbone constraint, so that *Ligulalepis, Dialipina* and *Janusiscus* were free to move into or out of the crown. To additionally assess the robustness of results to different phylogenetic and timescaling methods, an additional undated Bayesian analysis was performed in MrBayes3.2.6[44], and the post-burnin sample of trees was time-scaled using the "equal" method in the R function timePaleoPhy, package paleotree[45]. All three sets of trees

(BEAST2, BEAST2 constrained and MrBayes timescaled) were used for ancestral state reconstruction.

Four characters were used for ancestral state reconstructions, three of which were essentially the same as those found in the data matrix. These were *Oral dermal tubercles borne on jaw cartilages*, *Oral dermal tubercles in patterned rows (teeth)* and *Tooth whorls*. The latter two characters were changed from the form in the phylogenetic data matrix by recoding inapplicable (-) taxa as absent (0). This prevents illogical results (in particular the reconstruction of tooth whorls as present but oral tubercles as absent, even though tooth whorls are a form of oral tubercle). A fourth character was introduced for ancestral state reconstructions to assess the homology of osteichthyan, arthrodiran and ischnacanthid tooth rows. This character was formulated as *teeth, made of dentine, in organised rows and ankylosed to dermal jaw bones*. Due to its compound formulation it was not included in the original phylogenetic data matrix, which includes each of these aspects as a separate character. Brazeau & Friedman[46] demonstrated the importance of phylogenetically constrained comparative analysis, suggesting that oral tubercles and tooth whorls are ancestral for crown-gnathostomes. Our phylogentic analysis corroborates the ancestral condition of oral tubercles, but disagrees with the conclusion that tooth whorls are ancestral.

Ancestral state reconstructions were performed in BEAST1.10.2[47] with BEAGLE likelihood calculation library[37], using the post-burnin sample of trees from the three analyses detailed above. Characters were analysed with a strict clock, and a separate evolutionary rate was calculated for each of the four characters. An exponential prior with mean 0.1 was placed on the evolutionary rate. The analysis produced ancestral state reconstructions mapped onto the sample of trees[48] and a count of the number of state changes[49]. The analysis was run for 10 million generations, with 1000 trees saved. We tested symmetrical and asymmetrical models of trait evolution using Bayes factors. Marginal likelihoods were calculated using the stepping-stone method[50] with 100 steps, a chain length of 100,000 per step and alpha 0.3. The Bayes factor[51] support for asymmetrical models was 0.53 (“not worth more than a bare mention”), and we therefore chose the symmetrical model for interpretation. Results using the asymmetrical models are included in Extended Figure 3 for comparison.

Post-analysis processing was performed in R using the packages OutbreakTools[52], ape[53] and phangorn[54]. The state for each character at the crown gnathostome node in each tree of the post burn-in sample was assessed, producing posterior probabilities. We also assessed the homology of characters between osteichthyans and chondrichthyans (characters were said to be homologous if they were present at every node linking the two clades).

Transition counts are output by the BEAST analysis[49], but detailed inspection of the results reveals that some transitions are reconstructed incorrectly (for example a transition to a state on a branch leading to a taxon which lacks that state, and no reversal reconstructed on the same branch). Therefore the transition counts were also analysed in R using the ancestral state reconstruction at each node. Transitions were counted when a node had a state different to the immediately ancestral node. This provides a good estimate of the number of transitions, although it will be a slight underestimate as occasional double hits (i.e. two transitions in a single branch) will be missed.

Data availability

The data matrix is available in the Dryad data supplement. Sources for taxa and age ranges and the phylogenetic character list are available as supplementary information. Tomograms and surface files are archived in the University of Bristol Research Data Storage Facility at publication.

Code availability

Xml BEAST2 files, MrBayes nexus files, BEAST1 xml files and R scripts are available in the Dryad data supplement.

References

1 Smith, M. M. & Coates, M. I. Evolutionary origins of the vertebrate dentition: phylogenetic patterns and developmental evolution. *Eur J Oral Sci* **106**, 482-500, doi:10.1111/j.1600-0722.1998.tb02212.x (1998).

2 Botella, H., Blom, H., Dorka, M., Ahlberg, P. E. & Janvier, P. Jaws and teeth of the earliest bony fishes. *Nature* **448**, 583-586, doi:10.1038/nature05989 (2007).

3 Debiais-Thibaud, M. *et al.* Tooth and scale morphogenesis in shark: an alternative process to the mammalian enamel knot system. *Bmc Evol Biol* **15**, doi:ARTN 292 10.1186/s12862-015-0557-0 (2015).

4 Rasch, L. J. *et al.* An ancient dental gene set governs development and continuous regeneration of teeth in sharks. *Dev Biol* **415**, 347-370, doi:10.1016/j.ydbio.2016.01.038 (2016).

5 Smith, M. M., Fraser, G. J. & Mitsiadis, T. A. Dental Lamina as Source of Odontogenic Stem Cells: Evolutionary Origins and Developmental Control of Tooth Generation in Gnathostomes. *J Exp Zool Part B* **312b**, 260-280, doi:10.1002/jez.b.21272 (2009).

6 Tucker, A. S. & Fraser, G. J. Evolution and developmental diversity of tooth regeneration. *Semin Cell Dev Biol* **25**, 71-80, doi:10.1016/j.semcdb.2013.12.013 (2014).

7 Coates, M. I. *et al.* An early chondrichthyan and the evolutionary assembly of a shark body plan. *P Roy Soc B-Biol Sci* **285**, doi:10.1098/rspb.2017.2418 (2018).

8 Zhu, M. *et al.* A Silurian placoderm with osteichthyan-like marginal jaw bones. *Nature* **502**, 188-193, doi:10.1038/nature12617 (2013).

9 Giles, S., Friedman, M. & Brazeau, M. D. Osteichthyan-like cranial conditions in an Early Devonian stem gnathostome. *Nature* **520**, 82-U175, doi:10.1038/nature14065 (2015).
10 Smith, M. M. & Johanson, Z. Separate evolutionary origins of teeth from evidence in fossil jawed vertebrates. *Science* **299**, 1235-1236, doi:10.1126/science.1079623 (2003).
11 Denison, R. H. *Acanthodii*. (Gustav Fischer Verlag, 1979).
12 Smith, M. M. Vertebrate dentitions at the origin of jaws: when and how pattern evolved. *Evol Dev* **5**, 394-413, doi:DOI 10.1046/j.1525-142X.2003.03047.x (2003).
13 Blais, S. A., MacKenzie, L. A. & Wilson, M. V. H. Tooth-Like Scales in Early Devonian Eugnathostomes and the 'Outside-in' Hypothesis for the Origins of Teeth in Vertebrates. *Journal of Vertebrate Paleontology* **31**, 1189-1199, doi:10.1080/02724634.2011.607992 (2011).
14 Burrow, C. J., Newman, M., den Blaauwen, J., Jones, R. & Davidson, R. The Early Devonian ischnacanthiform acanthodian *Ischnacanthus gracilis* (Egerton, 1861) from the Midland Valley of Scotland. *Acta Geologica Polonica* **68**, 335–362, doi:10.1515/agp-2018-0008 (2018).
15 Burrow, C. J. Acanthodian fishes with dentigerous jaw bones: the Ischnacanthiformes and *Acanthodopsis*. *Fossils and Strata* **50**, 8-22 (2004).
16 Lindley, I. D. Acanthodian fish remains from the Lower Devonian Cavan Bluff Limestone (Murrumbidgee group), Taemas district, New South Wales. *Alcheringa* **24**, 11-35, doi:Doi 10.1080/03115510008619520 (2000).
17 Newman, M. J., Burrow, C. J., Blaauwen, den J. L. A new species of ischnacanthiform acanthodian from the Givetian of Mimerdalen, Svalbard. *Norwegian Journal of Geology* **99**, 1-13 (2019).
18 Gross, W. Über das Gebiss der Acanthodier und Placodermen. *Zoological Journal of the Linnean Society* **47**, 121-130 (1967).
19 Ørvig, T. Acanthodian dentition and its bearing on the relationships of the group. *Palaeontographica (Abt. A)* **143**, 119-150 (1973).
20 Smith, M. M., Coates, M. I. in *Major events of early vertebrate evolution* (ed P. E. Ahlberg) 223-240 (Taylor & Francis, 2001).
21 Donoghue, P. C. J. *et al.* Synchrotron X-ray tomographic microscopy of fossil embryos. *Nature* **442**, 680-683, doi:10.1038/nature04890 (2006).
22 Friedman, M. & Brazeau, M. D. A Reappraisal of the Origin and Basal Radiation of the Osteichthyes. *Journal of Vertebrate Paleontology* **30**, 36-56, doi:10.1080/02724630903409071 (2010).
23 Doeland, M., Couzens, A. M. C., Donoghue, P. C. J. & Rücklin, M. Tooth replacement in early sarcopterygians. *Roy Soc Open Sci* **6**, doi:ARTN 191173 10.1098/rsos.191173 (2019).
24 Jarvik, E. Middle and Upper Devonian Porolepiformes from East Greenland with special reference to *Glyptolepis groenlandica* n.sp. and a discussion on the structure of the head of Porolepiformes. *Medd. Groenland* **187**, 1-295 (1972).
25 Chen, D., Blom, H., Sanchez, S., Tafforeau, P. & Ahlberg, P. E. The stem osteichthyan *Andreolepis* and the origin of tooth replacement. *Nature* **539**, 237-241, doi:10.1038/nature19812 (2016).
26 Rücklin, M. *et al.* Development of teeth and jaws in the earliest jawed vertebrates. *Nature* **491**, 748-751, doi:10.1038/nature11555 (2012).
27 Clemen, G., Bartsch, P. & Wacker, K. Dentition and dentigerous bones in juveniles and adults of *Polypterus senegalus* (Cladistia, Actinopterygii). *Ann Anat* **180**, 211-221, doi:Doi 10.1016/S0940-9602(98)80076-9 (1998).
28 Chen, D. *et al.* Development of cyclic shedding teeth from semi-shedding teeth: the inner dental arcade of the stem osteichthyan *Lophosteus*. *R Soc Open Sci* **4**, 161084, doi:10.1098/rsos.161084 (2017).

29 Patterson, C. in *Problems of phylogenetic reconstruction. Systematics Association Special Volume 21* (eds K. A. Joysey & A. E. Friday) 21-74 (Academic Press, 1982).
30 King, B., Qiao, T., Lee, M. S. Y., Zhu, M. & Long, J. A. Bayesian Morphological Clock Methods Resurrect Placoderm Monophyly and Reveal Rapid Early Evolution in Jawed Vertebrates. *Syst Biol* **66**, 499-516, doi:10.1093/sysbio/syw107 (2017).
31 Andreev, P. *et al.* The systematics of the Mongolepidida (Chondrichthyes) and the Ordovician origins of the clade. *PeerJ* **4**, e1850, doi:10.7717/peerj.1850 (2016).
32 Rücklin, M., Giles, S., Janvier, P. & Donoghue, P. C. J. Teeth before jaws? Comparative analysis of the structure and development of the external and internal scales in the extinct jawless vertebrate *Loganellia scotica*. *Evol Dev* **13**, 523-532, doi:10.1111/j.1525-142X.2011.00508.x (2011).
33 White, E. I. The Old Red Sandstone of Brown Lee Hill and the adjacent area. II. Palaeontology. *Bulletin of the British Museum (Natural History) Geology* **5**, 245-310 (1961).
34 Stampanoni, M. *et al.* TOMCAT: A beamline for TOmographic Microscopy and Coherent rAdiology experimenTs. *Synchrotron Radiation Instrumentation, Pts 1 and 2* **879**, 848-851, doi:doi.org/10.1063/1.2436193 (2007).
35 Maisey, J. G. *et al.* in *Evolution and Development of FIshes* (eds Z. Johanson, C. J. Underwood, & M. Richter) 87-109 (Cambridge University Press, 2018).
36 Bouckaert, R. *et al.* BEAST 2.5: An advanced software platform for Bayesian evolutionary analysis. *Plos Comput Biol* **15**, doi:ARTN e1006650 10.1371/journal.pcbi.1006650 (2019).
37 Ayres, D. L. *et al.* BEAGLE: An Application Programming Interface and High-Performance Computing Library for Statistical Phylogenetics. *Syst Biol* **61**, 170-173, doi:10.1093/sysbio/syr100 (2012).
38 Lewis, P. O. A likelihood approach to estimating phylogeny from discrete morphological character data. *Syst Biol* **50**, 913-925, doi:10.1080/106351501753462876 (2001).
39 Gavryushkina, A., Welch, D., Stadler, T. & Drummond, A. J. Bayesian Inference of Sampled Ancestor Trees for Epidemiology and Fossil Calibration. *Plos Comput Biol* **10**, doi:ARTN e100391910.1371/journal.pcbi.1003919 (2014).
40 Drummond, A. J., Ho, S. Y. W., Phillips, M. J. & Rambaut, A. Relaxed phylogenetics and dating with confidence. *Plos Biol* **4**, 699-710, doi:ARTN e88 10.1371/journal.pbio.0040088 (2006).
41 Rambaut, A., Suchard, M. A., Xie, D. & Drummond, A. J. *Tracer v1.6.*, <http://beast.bio.ed.ac.uk/Tracer> (2014).
42 Warren, D. L., Geneva, A. J. & Lanfear, R. RWTY (R We There Yet): An R Package for Examining Convergence of Bayesian Phylogenetic Analyses. *Mol Biol Evol* **34**, 1016-1020, doi:10.1093/molbev/msw279 (2017).
43 King, B. Which morphological characters are influential in a Bayesian phylogenetic analysis? Examples from the earliest osteichthyans. *Biol Letters* **15**, doi:ARTN 20190288 10.1098/rsbl.2019.0288 (2019).
44 Ronquist, F. *et al.* MrBayes 3.2: Efficient Bayesian Phylogenetic Inference and Model Choice Across a Large Model Space. *Syst Biol* **61**, 539-542, doi:10.1093/sysbio/sys029 (2012).
45 Bapst, D. W. paleotree: an R package for paleontological and phylogenetic analyses of evolution. *Methods Ecol Evol* **3**, 803-807, doi:10.1111/j.2041-210X.2012.00223.x (2012).
46 Brazeau, M. D. & Friedman, M. The characters of Palaeozoic jawed vertebrates. *Zoological Journal of the Linnean Society* **170**, 779-821, doi:10.1111/zoj.12111 (2014).
47 Suchard, M. A. *et al.* Bayesian phylogenetic and phylodynamic data integration using BEAST 1.10. *Virus Evol* **4**, doi:UNSP vey016 10.1093/ve/vey016 (2018).

48 Lemey, P., Rambaut, A., Drummond, A. J. & Suchard, M. A. Bayesian Phylogeography Finds Its Roots. *Plos Comput Biol* **5**, doi:ARTN e100052010.1371/journal.pcbi.1000520 (2009).
49 Minin, V. N. & Suchard, M. A. Counting labeled transitions in continuous-time Markov models of evolution. *J Math Biol* **56**, 391-412, doi:10.1007/s00285-007-0120-8 (2008).
50 Xie, W., Lewis, P. O., Fan, Y., Kuo, L. & Chen, M. H. Improving marginal likelihood estimation for Bayesian phylogenetic model selection. *Syst Biol* **60**, 150-160, doi:10.1093/sysbio/syq085 (2011).
51 Kass, E. R. R., A. E. Bayes Factors. *Journal of the American Statistical Association* **90**, 773-795 (1995).
52 Jombart, T. *et al.* OutbreakTools: A new platform for disease outbreak analysis using the R software. *Epidemics-Neth* **7**, 28-34, doi:10.1016/j.epidem.2014.04.003 (2014).
53 Paradis, E., Claude, J. & Strimmer, K. APE: Analyses of Phylogenetics and Evolution in R language. *Bioinformatics* **20**, 289-290, doi:10.1093/bioinformatics/btg412 (2004).
54 Schliep, K. P. phangorn: phylogenetic analysis in R. *Bioinformatics* **27**, 592-593, doi:10.1093/bioinformatics/btq706 (2011).

Acknowledgements

We thank S. Bengtson, D. Murdock for help at the TOMCAT beamline. We also want to thank Emma Bernard (Natural History Museum) for access to collections and for facilitating loan of specimens. The study was funded by EU FP7 Marie-Curie Intra-European Fellowship (to M.R. and P.C.J.D.), Natural Environmental Research council Grant NE/G016623/1 (to P.C.J.D.) and NWO (VIDI 864.14.009, to M.R.). We acknowledge the Paul Scherrer Institut, Villigen, Switzerland for provision of synchrotron radiation beamtime at the TOMCAT (X02DA) beamline of the SLS (to P.C.J.D. and S. Bengtson).

Author contributions

M.R. and P.C.J.D. designed initial research; M.R., J.A.C., P.C.J.D. and F.M. performed scans, M.R. and J.A.C. segmented tomograms, B.K. produced the phylogenetic data matrix performed the phylogenetic analysis and ancestral state reconstruction. M.R. and P.D. drafted the manuscript to which all authors contributed.

Competing interests statement

The authors declare no competing interests.

Additional information

Supplementary information is available for this paper. Correspondence and requests for materials should be addressed to M.R. (martin.rucklin@naturalis.nl) and P.D. (phil.donoghue@bristol.ac.uk). Reprints and permissions information is available at www.nature.com/reprints.

453

454 **Figure Legends**

455

456 **Figure 1 | Jaw bones and marginal dentition of ischnacanthid acanthodians.** Mandible
457 of *Ischnacanthus kingi* lateral view of complete specimen in rock (**a)** NHMUK PV P.15362.
458 Mandible of ischnacanthid acanthodian NRM-PZ P. 9449 lateral view (**b**) and dorsal view (**c**)
459 of complete ossified bone and teeth. Detailed lateral view showing the tooth addition in the
460 lateral row, indicated by arrows (**d)**, and detail of the spheritic mineralisations (**e**). Detailed
461 dorsal view with teeth separated by growth arrest line, indicated by arrows (**f**). Distal most
462 tooth of the lingual row overlaps tooth within the lateral row (**g**). Overgrowth of teeth at the
463 centre of ossification and initial sequential addition, indicated by arrow (**h**). Largest and last
464 added medial tooth showing a hypermineralised layer, we interpret as enameloid, forming the
465 proximal ridge and the smaller marginal cusplets and dentine infilling the pulp cavity (**i**).
466 Scale bar in (**a)** represents 4.3 mm, 270 µm (**b**, **c**), 107 µm (**d**), 61 µm (**e**), 156 µm (**f**), xx µm
467 (**g**), 21 µm (**h**) and 50 µm (**i**).

468

469 **Figure 2 | Surface and reconstructed growth of marginal tooth rows on an**
470 **ischnacanthid acanthodian jawbone.** Jawbone NRM-PZ P. 9449 Early Devonian, Canada.
471 Lateral view of the surface (**a**) and reconstructed addition of teeth (**b**). Occlusal view of the
472 surface (**c**) and reconstructed addition of teeth (**c**). Colours of the nested boxes reflect the
473 successive stages of tooth development. Scale bar represents 220 µm, prox, proximal; dist,
474 distal; ling, lingual; lab, labial.

475

476 **Figure 3 | Virtual development of teeth on an ischnacanthid acanthodian jawbone.**
477 Marginal tooth rows of NRM-PZ P. 9449 Early Devonian, Canada. Labelled sclerochronology
478 of the teeth in possible sequence of addition in oral (**a**) and labial view (**b**). Colours of the
479 nested boxes reflect the successive stages of tooth development. Scale bar represents 150
480 µm. Arrow indicates sequence of addition; prox, proximal; dist, distal; ling, lingual; lab, labial.

481

482 **Figure 4 | Tooth whorl of an ischnacanthid acanthodian.** Tooth whorl NRM-PZ P. 15908
483 (**a** - **c**), lateral view complete bone and teeth (**a**), virtual section showing tooth and base
484 developing synchronous separated from successive teeth by a growth arrest line (**b**) and
485 virtual section through second tooth and side teeth (**c**). Scale bar equals 120 µm in (**a**), 60
486 µm in (**b**) and 42 µm in (**c**).

487

488 **Figure 5 | 50% majority rule consensus tree from a tip-dated Bayesian analysis**,
489 annotated with ancestral state reconstructions for oral tubercles. Yellow represents absent

and blue represents present; branch widths proportional to posterior probability for reconstructed state. Arrows indicate taxon ages that extend beyond the range displayed on the figure.

Figure 6 | 50% majority rule consensus tree from a tip-dated Bayesian analysis, annotated with ancestral state reconstructions for ankylosed tooth rows (**a**) and tooth whorls (**b**). Branch widths proportional to posterior probability of reconstructed state. Arrows indicate taxon ages that extend beyond the range displayed on the figure.

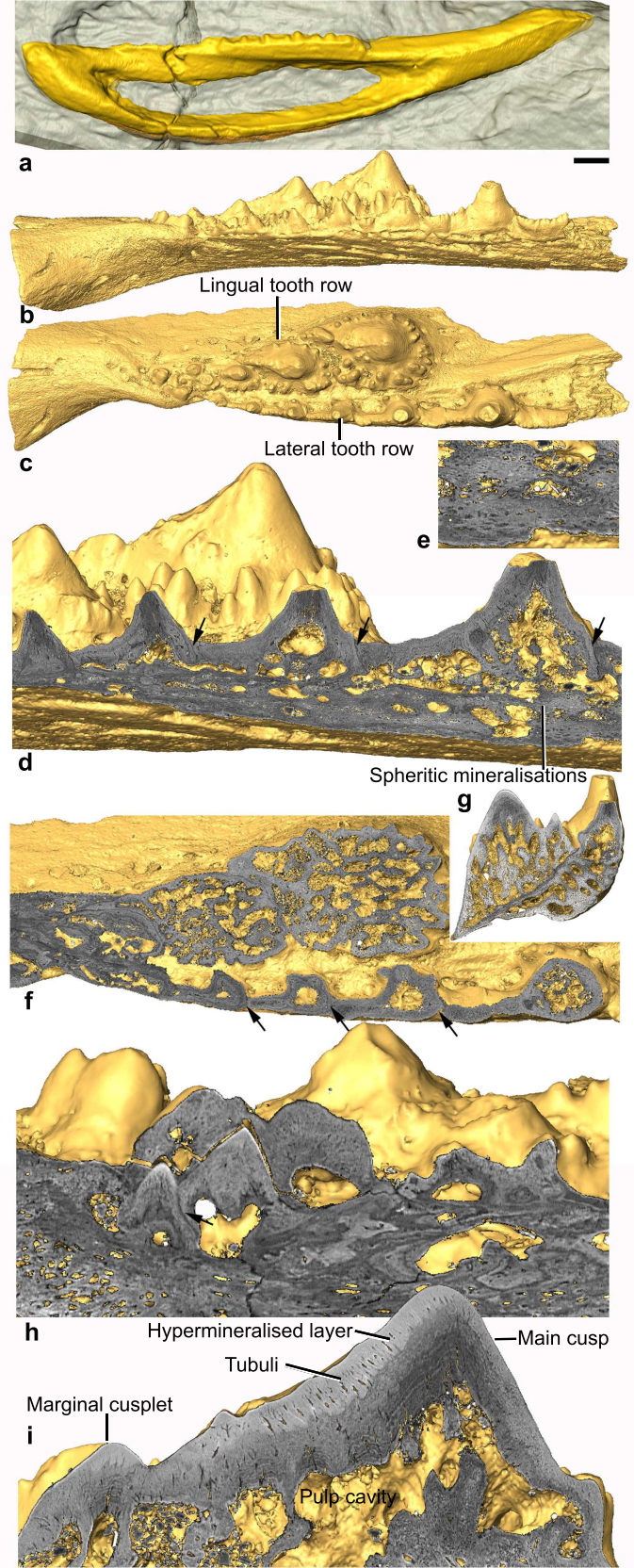
a
Lingual tooth row
b
Lateral tooth row
c
e
d
Spheritic mineralisations
g
f
h
Hypermineralised layer
Main cusp
Tubuli
Marginal cusplet
i
Pulp cavity

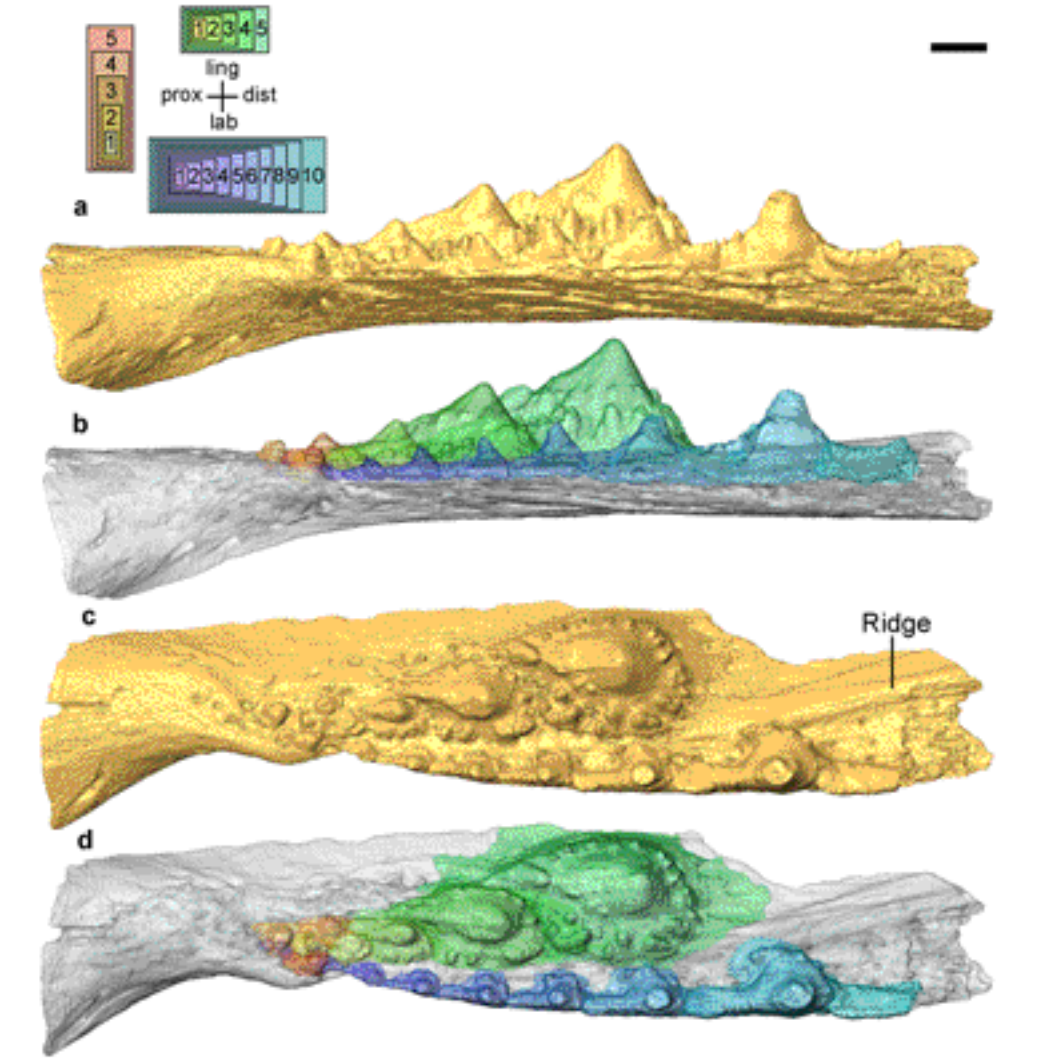
5
4
3
2
1
1 2 3 4 5
ling
prox
dist
lab
1 2 3 4 5 6 7 8 9 10
a
b
c
Ridge
d

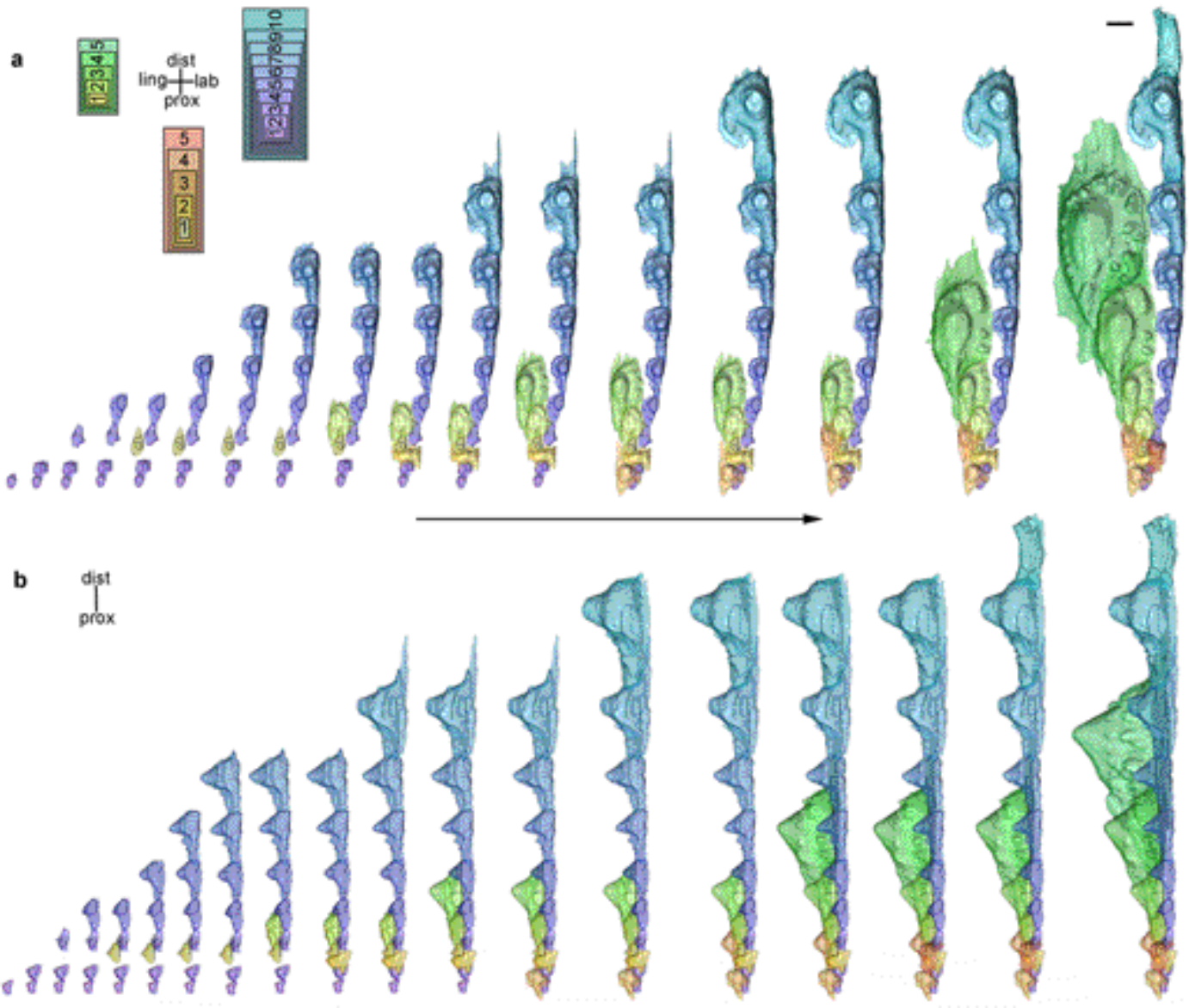
a
dist
ling
lab
prox
1 2 3 4 5
1 2 3 4 5 6 7 8 9 10
5
4
3
2
1
b
dist
prox

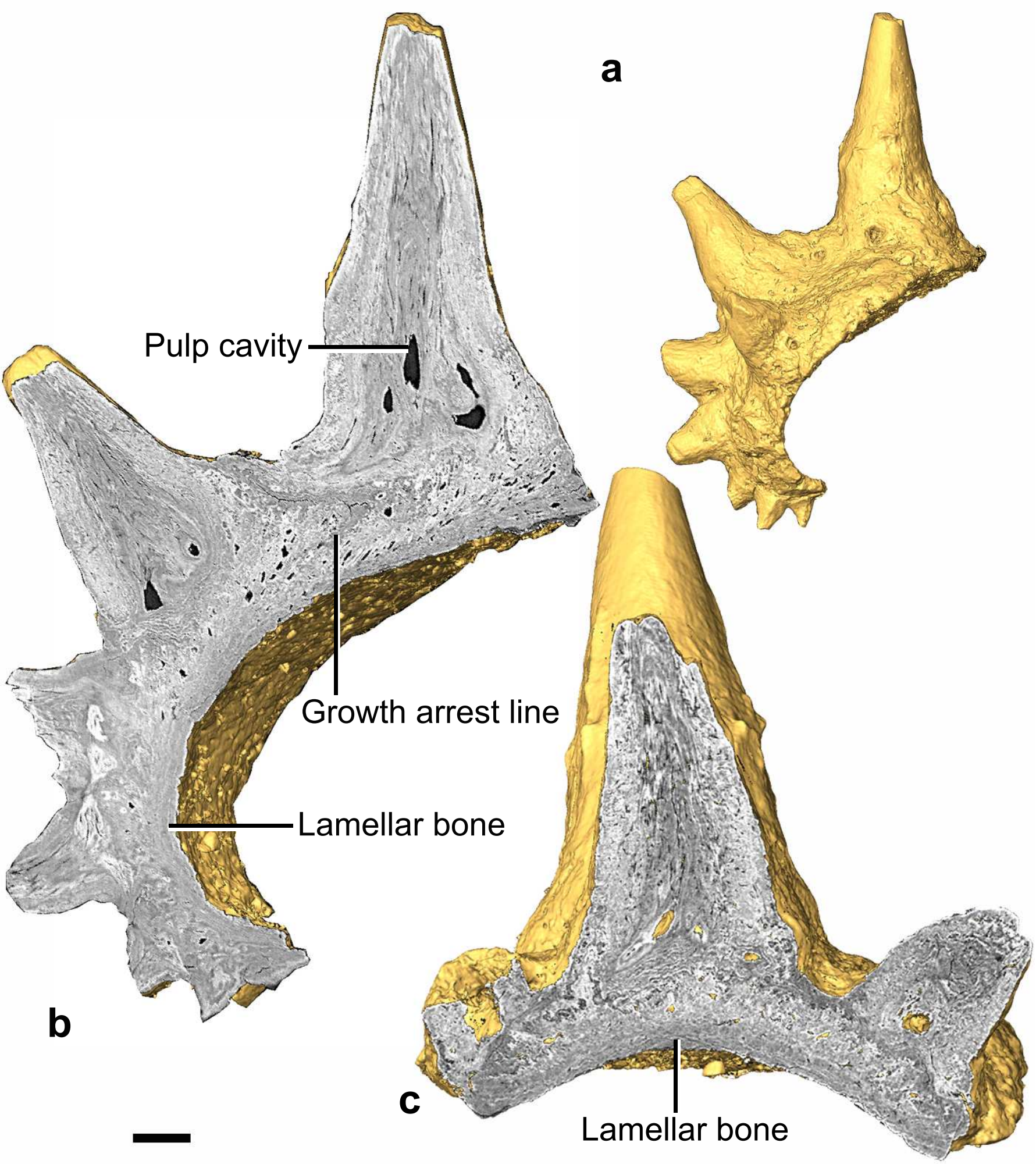
a
Pulp cavity
Growth arrest line
Lamellar bone
b
c
Lamellar bone

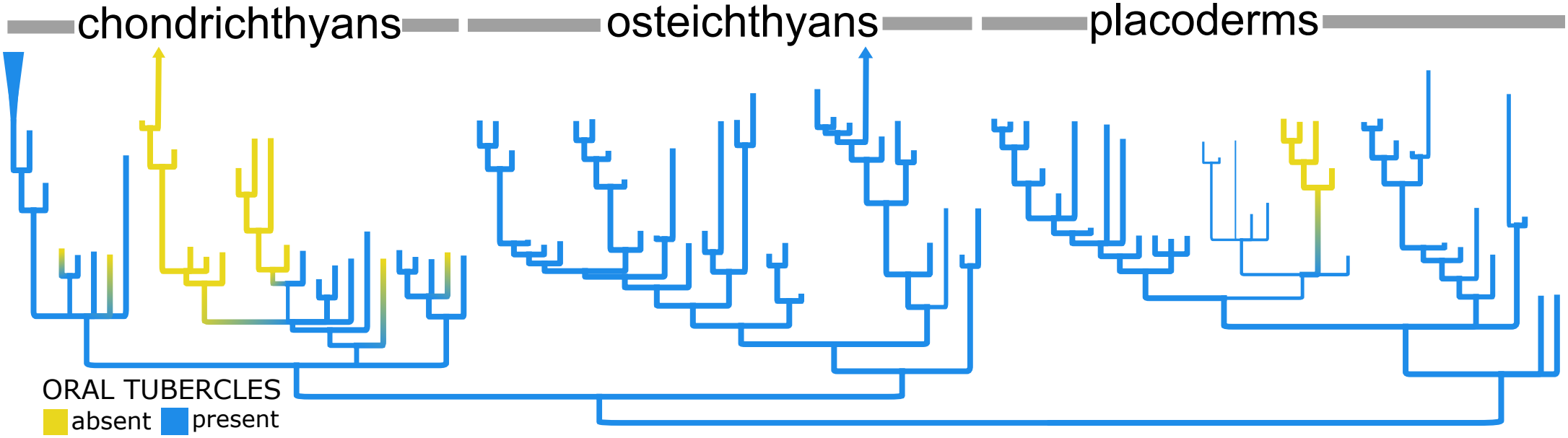
chondrichthyans
osteichthyans
placoderms
ORAL TUBERCLES
absent
present

ANKYLOSED TOOTH ROWS

absent

present

TOOTH WHORLS

Gladbachus
Doliodus
Lupopsyrus
Obtusacanthus
Brochoadmones
Kathemacanthus
Pucapampella
Homalacanthus
Acanthodes
Cheiracanthus
Promesacanthus
Mesacanthus
Cassidiceps
Diplacanthus
Culmacanthus
Milesacanthus
Gladiobranchus
Tetanopsyrus
Nerepisacanthus
Poracanthodes
Ischnacanthus
Latviacanthus
Euthacanthus
Vernicomacanthus
Parexus
Climatius
Brachyacanthus
Ptomacanthus
Rhinodipterus
Chirodipterus
Dipterus
Diabolepis
Youngolepis
Powichthys
Gogonasus
Eusthenopteron
Osteolepis
Kenichthys
Tungsenia
Porolepis
Glyptolepis
Styloichthys
Qingmenodus
Onychodus
Miguashaia
Diplocercides
Psarolepis
Achoania
Guiyu
Raynerius
Moythomasia
Mimipiscis
Kentuckia
Howqualepis
Cheirolepis
Cheirolepis
Meemannia
“Ligulalepis”
Janusiscus
Dialipina
Incisoscutum
Eastmanosteus
Compagopiscis
Coccosteus
Parabuchanosteus
Holonema
Buchanosteus
Cowralepis
Groenlandaspis
Dicksonosteus
Sigaspis
Kujdanowiaspis
Lehmanosteus
Quasipetalichthys
Macropetalichthys
Eurycaraspis
Lunaspis
Shearsbyaspis
Materpiscis
Austroptyctodus
Campbellodus
Rhamphodopsis
Diandongpetalichthys
Bothriolepis
Bothriolepis
Microbrachius
Pterichthyodes
Remigolepis
Parayunnanolepis
Yunnanolepis
Brindabellaspis
Romundina
Jagorina
Gemuendina
Entelognathus
Qilinyu

acanthodians

sarcopterygians

arthrodires

chondrichthyans

osteichthyans

placoderms